Journal of Applied Electrochemistry (2018) 48:1189–1195
https://doi.org/10.1007/s10800-018-1211-5

RESEARCH ARTICLE

PPy enhanced Fe, W Co-doped Co_3O_4 free-standing electrode for highly-efficient oxygen evolution reaction

Qingzhao Hu[1] · **Yan Liu**[1] · **Longtao Ma**[2] · **Xuming Zhang**[1] · **Haitao Huang**[1]

Received: 20 March 2018 / Accepted: 15 May 2018 / Published online: 22 May 2018

Abstract

Electrochemical catalysts for the oxygen evolution reaction (OER) play a key role in highly-efficient water splitting and many other important energy conversion applications. Transition metal oxides are promising OER catalysts. In this work, Fe, W co-doped Co_3O_4 was grown on carbon fiber cloth ($FeWCo_3O_4$/CFC) and polypyrrole (PPy)/carbon fiber cloth ($FeWCo_3O_4$/PPy/CFC) through a simple anodic electrodeposition method. The $FeWCo_3O_4$/CFC free-standing electrode reached an electrocatalytic current density of 30.7 mA cm^{-2} at 400 mV overpotential with a Tafel slope of 177 mV dec^{-1}. The PPy can serve as conductive binder and improve the contact between $FeWCo_3O_4$ and substrate. The resulting $FeWCo_3O_4$/PPy/CFC free-standing electrode reached an electrocatalytic current density of 36.2 mA cm^{-2} at 400 mV overpotential with a Tafel slope of 163 mV dec^{-1}. The $FeWCo_3O_4$/PPy/CFC free-standing electrode shows low electric resistance and is able to catalyze OER at 10 mA cm^{-2} for 12 h without obvious decay under the optimized electrodeposition conditions. This study provides new insight for design and synthesis of highly-efficient OER catalyst.

Graphical Abstract

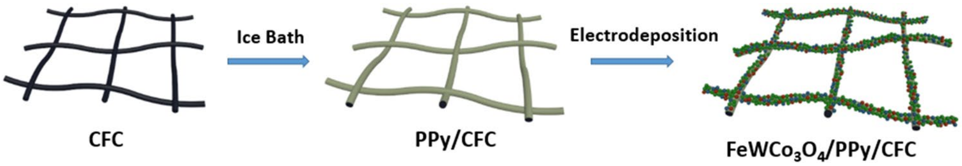

Keywords Oxygen evolution reaction · Free-standing electrode · Electrodeposition · PPy

1 Introduction

Energy crisis and global warming have raised worldwide interest in developing environment-friendly energy sources [1–3]. Alternatives to fossil fuels are significant to help reduce green-house effect and air pollution [3, 4]. Hydrogen, which is recognized as a clean and renewable energy source, possesses great potential to become the next generation energy source [2, 3]. Hydrogen production through methane or coal in industry involves enormous carbon dioxide emission [5]. While mass production of hydrogen by electrolysis with high efficiency remains laborious due to the sluggish kinetics of oxygen evolution reaction (OER) in water splitting [5, 6]. Superb catalyst which can promote the oxygen evolution is crucial to the production of hydrogen through water splitting. The state-of-art catalysts RuO_2 and IrO_2

Electronic supplementary material The online version of this article (https://doi.org/10.1007/s10800-018-1211-5) contains supplementary material, which is available to authorized users.

✉ Haitao Huang
aphhuang@polyu.edu.hk

[1] Department of Applied Physics, The Hong Kong Polytechnic University, Hung Hom, Kowloon 999077, Hong Kong, China

[2] Department of Materials Science and Engineering, City University of Hong Kong, Kowloon 999077, Hong Kong, China

suffer from high cost and low abundance [7]. Catalyst fabricated with earth-abundant elements is therefore needed to surmount the reaction obstacles and increase the efficiency.

Recent years have seen huge efforts focused on the synthesis of transition metal-based materials [8–15], such as transition metal oxides and transition metal (oxy)hydroxides (CoOOH [16], NiCoFe layered triple hydroxide [17], FeCoW oxyhydroxide [9]), transition metal phosphides (CoP [18], NiP [19]), metal–organic frameworks (NiCo bimetal–organic framework [20]) and composites (NiFe layered double hydroxide–graphene oxide [8]). Some OER catalysts derived from Co_3O_4 have been reported, such as Au@Co_3O_4 core–shell nanocrystals [21] and graphene–Co_3O_4 nanocomposite [22]. However, the synthesis of Au@Co_3O_4 core–shell nanocrystals involves noble metal, which is adverse to industry application. The synthesis method of graphene–Co_3O_4 nanocomposite is complicated and high temperature calcination is also required. In addition, binder such as Nafion is needed for the fabrication of electrodes using powdered catalysts [20, 23]. Therefore, the fabrication of free-standing electrode with highly-efficient OER catalysts that consist of earth-abundant elements is attractive and challenging.

There are two general approaches to the development of an effective catalyst: improving the intrinsic property of each site or increasing the amount of effective sites. Intrinsic property can be enhanced by tuning binding energies of reaction intermediates. Morphology design contributes to the number of effective active sites [15]. A recent study predicted the superior intrinsic catalytic performance of FeCoW oxyhydroxide by calculating the corresponding binding energies of the intermediates using density functional theory (DFT+U) [9]. Non-3d high-valency metals such as tungsten can modulate 3d metal oxides to provide optimized adsorption energies and electronic structure for highly efficient OER. Cobalt-based composites supported on carbon fiber substrate are shown to be highly-efficient electrochemical catalysts, which may result from high electric conductivity and synergistic effect between cobalt oxide/cobalt and carbon substrate [24, 25]. It is reported that PPy/carbon structure can increase the metal availability for electrode reaction [26]. Meanwhile, PPy and cobalt can form Co–N active sites with enhanced electrochemical property [27, 28]. Therefore, a highly-efficient OER catalytic electrode is expected through the fabrication of FeCoW catalyst supported by PPy/CFC substrate.

Herein, $FeWCo_3O_4$/PPy/CFC free-standing electrode was synthesized through a simple electrodeposition method and showed efficient OER catalytic performance. The $FeWCo_3O_4$/PPy/CFC electrodes achieved a higher current density (36.2 mA cm^{-2}) than $FeWCo_3O_4$/CFC (30.7 mA cm^{-2}) at an overpotential of 400 mV. The PPy was demonstrated to improve the contact between active material and substrate, which enables better OER electrocatalytic performance of $FeWCo_3O_4$/PPy/CFC electrode than that of $FeWCo_3O_4$/CFC electrode.

2 Experimental section

Carbon fiber clothes (CFC) were firstly washed with deionized water (DI water) and acetone several times, then immersed into dilute nitric acid for 24 h to remove the surface impurities. Thereafter, the CFC were washed with DI water and dried at 60 °C in oven for 2 h before use.

2.1 PPy grown on CFC (PPy/CFC)

Pyrrole (1 mL) was firstly dissolved into DI water (50 mL). Then ammonium persulfate (1 g) and sodium *p*-toluenesulfonate (1 g) were added into the above solution. Thereafter the solution was placed into ice bath and stirred for 10 min. CFC were put into the solution for 2 h polymerization to obtain PPy/CFC, which was then washed with DI water several times and dried in oven at 60 °C for 2 h.

2.2 Fe, W co-doped Co_3O_4 grown on PPy/CFC ($FeWCo_3O_4$/PPy/CFC)

Trisodium citrate dehydrate (14.75 g), boric acid (2.56 g), sodium tungstate (19.5 g), iron(II) chloride tetrahydrate (0.49 g) and cobalt chloride hexahydrate (0.59 g) were dissolved into DI water (250 mL). Phosphoric acid (1.9 mL, 85 wt%) was added into the above solution. Then the solution was put under ultrasonic condition for 1 h. After that, the solution was stirred for 12 h to become homogenous. The above solution was added into an electrochemical cell with PPy/CFC as anode, Pt plate as cathode. Electrodeposition was conducted under a constant current density of 40 mA cm^{-2} for 2 h under 60 °C water bath condition. The deposited $FeWCo_3O_4$/PPy/CFC was washed with DI water and ethanol for several times. Scheme 1 shows the synthesis of $FeWCo_3O_4$/PPy/CFC schematically.

2.3 Fe, W co-doped Co_3O_4 grown on CFC ($FeWCo_3O_4$/CFC)

The method used was similar to that of the deposition of $FeWCo_3O_4$/PPy/CFC with CFC being the anode instead of PPy/CFC.

2.4 Characterizations

Scanning electron microscope (SEM, TM 3000, Hetachi, Janpan) and transmission electron microscopy (TEM, JOEL JEM-2010, Janpan) were used for microstructure

Scheme 1 Schematic illustration of synthesis of $FeWCo_3O_4$/PPy/CFC

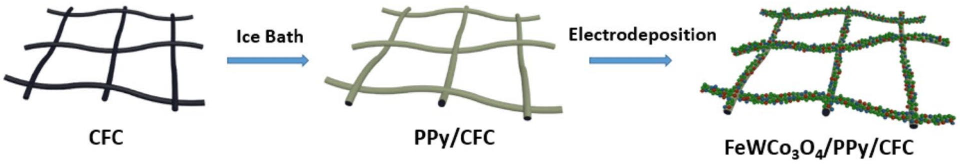

and morphology characterizations. X-ray diffraction (XRD, Rigaku D/max IIIA, Cu Kα, $\lambda = 0.15418$ nm, Japan) was used for crystalline structure analysis. Raman spectrum was conducted on a HORIBA Raman spectrometer at 488 nm. X-ray photoelectron spectroscopy (XPS, Thermo Microlab 350) was used to study the surface composition of $FeWCo_3O_4$ inside an ultrahigh vacuum system.

2.5 Electrochemical measurements

Linear sweep voltammetry, cyclic voltammetry (CV), electrochemical impedance spectroscopy (EIS, 0.01–1000 k Hz frequency) and chronopotentiometric tests were performed on an electrochemical workstation (Solartron Analytical 1470E). A classical three-electrode configuration was used with Pt plate as counter electrode and saturated calomel electrode (SCE) as reference electrode. The measurement was conducted in 1 mol L^{-1} KOH solution and the polarization curve was tested at a scan rate of 2 mV s^{-1}.

3 Results and discussion

Figure 1a–c displays the SEM images of $FeWCo_3O_4$ on the CFC without PPy modification under different magnifications. It can be seen clearly that the deposited $FeWCo_3O_4$ layer has many cracks and is easy to be peeled off, leading to poor contact between $FeWCo_3O_4$ layer and CFC fiber and resulting in mechanical instability of the $FeWCo_3O_4$/CFC structure. In contrast, when the PPy modified CFC is used as substrate, the contact between $FeWCo_3O_4$ and substrate is significantly improved (Fig. 1d–f). No cracks can be

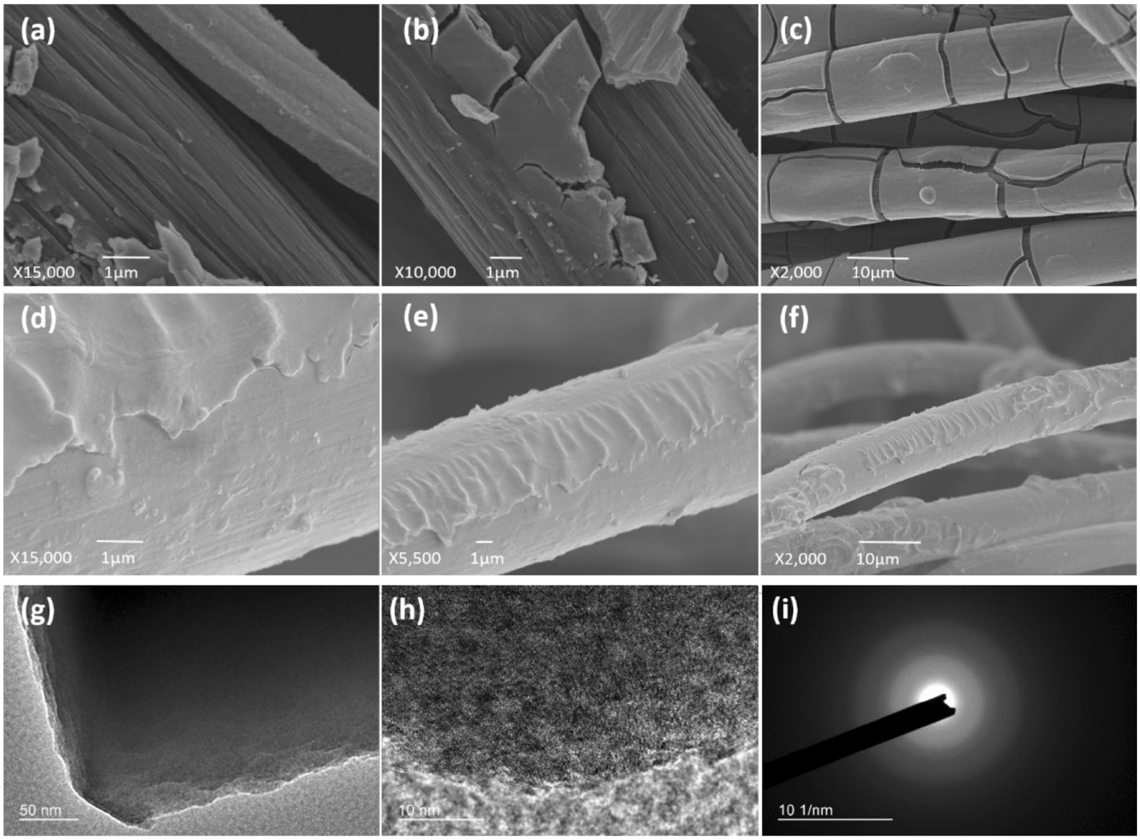

Fig. 1 **a–c** SEM images of $FeWCo_3O_4$/CFC with different magnifications. **d–f** SEM images of $FeWCo_3O_4$/PPy/CFC with different magnifications. **g–i** TEM image, HRTEM image and corresponding SAED pattern of $FeWCo_3O_4$ layer stripped from $FeWCo_3O_4$/PPy/CFC

identified at the surface of the $FeWCo_3O_4$/PPy/CFC structure. The strong adhesion between $FeWCo_3O_4$ and substrate prevents the loss of effective active sites and leads to stable catalytic performance.

The lack of distinct lattice fringes in TEM images (Fig. 1g, h) and the diffuse rings in the corresponding selected area electron diffraction (SAED) pattern (Fig. 1i) reveal that the thin $FeWCo_3O_4$ nanosheets are amorphous.

Only diffraction peaks of the CFC substrate (JCPDS Card No. 41-1487) can be observed in the XRD pattern of the electrodeposited $FeWCo_3O_4$ (Fig. 2a), which further confirms the amorphous structure of the $FeWCo_3O_4$ layer. The Raman spectrum reveals the existence of Co_3O_4 as shown in Fig. 2b. The observed 188, 466, 509, 601, and 671 cm^{-1} peaks agree well with pure spinel structure of Co_3O_4 [29]. The two peaks at 1360 and 1590 cm^{-1} belong to the CFC substrate.

XPS spectrum provides the detailed information of valence states. Co in Co_3O_4 is actually in a mixed oxidation state of Co^{2+} and Co^{3+}. As shown in Fig. 3a, Co consists of +2 and +3 values which is consistent with Co_3O_4 composition indicated by Raman spectra. The peaks at 780.48 and 782.03 eV belong to Co $2p_{3/2}$ region of Co^{3+} and Co^{2+}, respectively. The corresponding satellite peak of Co $2p_{3/2}$ is observed at 786.23 eV. Peaks of Co $2p_{1/2}$ are also observed at 795.48 eV for Co^{3+} and 797.23 eV for Co^{2+}, accompanied with a satellite peak (denoted as Sat.) at 803.98 eV.

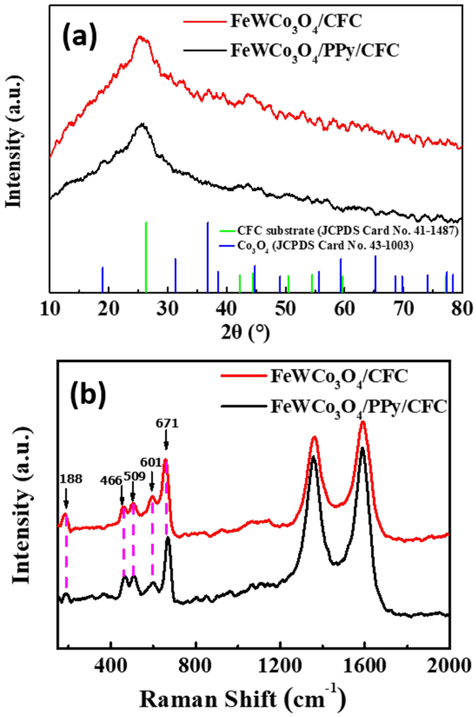

Fig. 2 **a** XRD patterns and **b** Raman spectra of electrodeposited $FeWCo_3O_4$/PPy/CFC and $FeWCo_3O_4$/CFC

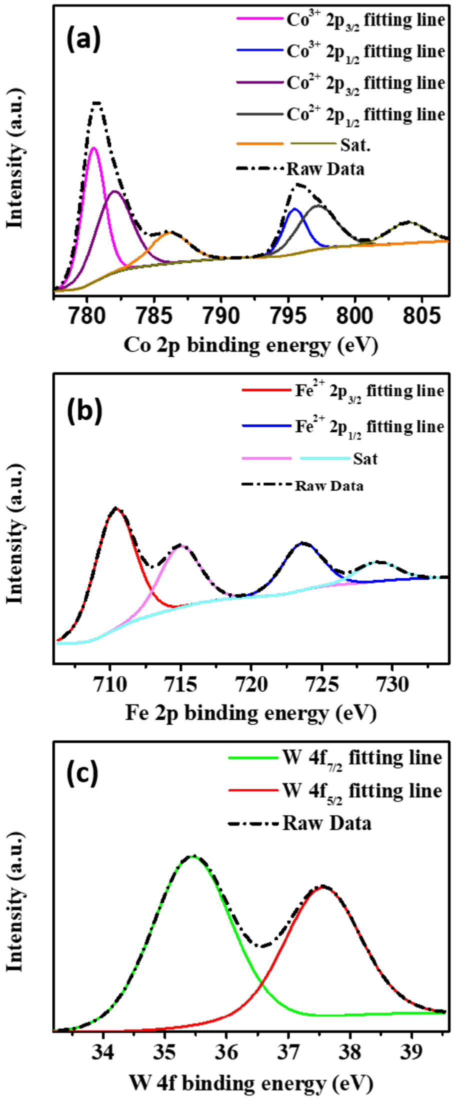

Fig. 3 Measurements of **a** Co 2p XPS, **b** Fe 2p XPS, **c** W 4f XPS of $FeWCo_3O_4$/PPy/CFC

Figure 3b shows the Fe^{2+} $2p_{3/2}$ peak at 710.43 eV, with a satellite peak at 715.03 eV. Peaks at 723.73 and 729.03 eV belong to Fe^{2+} $2p_{1/2}$ and the corresponding satellite peaks, respectively. The XPS results reveal that Fe exists only in the valence state of Fe^{2+}. As shown in Fig. 3c, the peaks at 35.45 and 37.58 eV belong to W $4f_{7/2}$ and W $4f_{5/2}$ of W^{6+}, respectively, indicating that only W^{6+} exists in the deposited $FeWCo_3O_4$. EDS measurement (Fig. S1, Supporting Information) shows that the sample contains the major metal element of Co, with only small amounts Fe and W.

The OER electrocatalytic property was tested in 1.0 M KOH alkaline media at a scan rate of 2 mV s^{-1} with SCE as reference electrode and Pt plate as counter electrode. The potential measured with the SCE reference electrode can be converted into the potential with respect to the reversible hydrogen electrode (RHE) according to the following equation:

$$E(RHE) = E(SCE) + (0.059\ pH + 0.242)\ V$$

The polarization curves of $FeWCo_3O_4$/PPy/CFC and $FeWCo_3O_4$/CFC are shown in Fig. 4a. The peaks of the polarization curves near 1.25 V (vs. RHE) may be associated with the reaction: $Co_3O_4 + H_2O + OH^- \rightarrow 3CoOOH + e^-$. The conductive CoOOH formed on the surface of the electrode is found to be active to the OER [30]. The current density of $FeWCo_3O_4$/PPy/CFC is higher than $FeWCo_3O_4$/CFC beyond 1.55–1.65 V (vs. RHE). This can be explained by the function of PPy which can serve as a conductive binder to improve the conductivity. CV measurement indicates the existence of additional redox current from 1.25 to 1.50 V versus RHE (Figs. S3, S4 Supporting Information). To avoid the disturbance of this redox current, the current density at an overpotential of 400 mV (1.63 V) is used to compare the electrocatalytic performance of the two samples. It can be seen that the $FeWCo_3O_4$/PPy/CFC free-standing electrode reaches a higher current density of 36.2 mA cm^{-2} than the $FeWCo_3O_4$/CFC (30.7 mA cm^{-2}) does at an overpotential of 400 mV. The Tafel slope of $FeWCo_3O_4$/PPy/CFC (163 mV dec^{-1}) is slightly lower than that of $FeWCo_3O_4$/CFC (177 mV dec^{-1}) (Fig. 4b), which can be ascribed to the enhanced electron transfer from PPy. EIS test indicates the lower resistance of $FeWCo_3O_4$/PPy/CFC than that of $FeWCo_3O_4$/CFC (Fig. 4c). The stability of $FeWCo_3O_4$/PPy/CFC and $FeWCo_3O_4$/CFC is tested by applying a constant current density of 10 mA cm^{-2} for 12 h (Fig. 4d). The catalytic performance is stable without obvious decay for 12 h. Electrodeposition time is an important factor to influence the catalytic performance of $FeWCo_3O_4$/PPy/CFC. When the deposition time is 2 h, the sample shows the best electrocatalytic performance (Fig. S2, Supporting Information). The difference in the electrocatalytic performance of samples deposited with different deposition time periods may result from two factors: the number of active sites and electron transportation. The sample with too short deposition time (1 h) may suffer from fewer active sites. However, the sample with too long deposition time (3 h) has thick layers which impedes the electron transfer.

4 Conclusion

By using a simple anodic electrodeposition method, amorphous Co_3O_4 co-doped with Fe, W were grown on PPy/CFC substrate. The $FeWCo_3O_4$/PPy/CFC electrode with additional PPy layer possesses better OER electrocatalytic

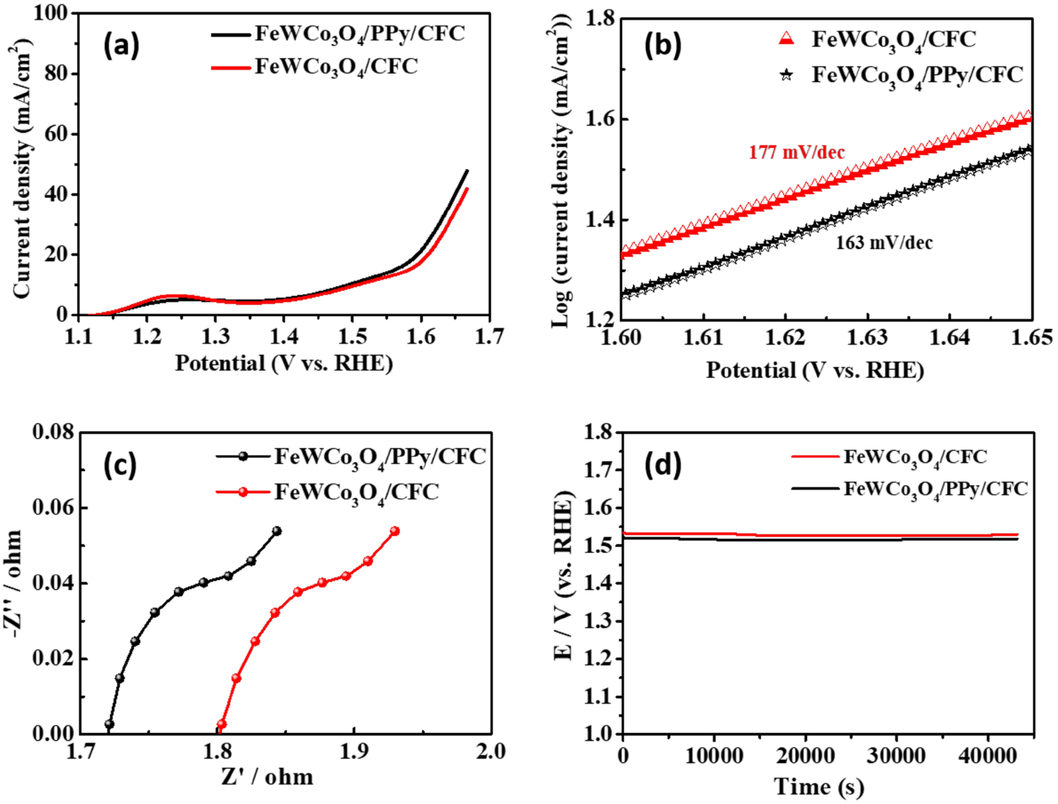

Fig. 4 **a** Polarization curve, **b** Tafel plot, **c** EIS plot and **d** chronopotentiometric curve of $FeWCo_3O_4$/PPy/CFC and $FeWCo_3O_4$/CFC

activities than $FeWCo_3O_4$/CFC. PPy can serve as conductive binder to improve the surface contact between $FeWCo_3O_4$ active material and the substrate. CFC is flexible and highly conductive, which is also stable at anodic condition during the deposition of $FeWCo_3O_4$. The synthesized $FeWCo_3O_4$/PPy/CFC free-standing electrode exhibits high OER catalytic performance with a current density of 36.2 mA cm^{-2} at an overpotential of 400 mV, and a Tafel slope of 163 mV dec^{-1}. This study provides new insight for design and synthesis of highly-efficient OER catalyst.

Acknowledgements This work was supported by the Hong Kong Polytechnic University (Project No. RUKQ).

References

1. Chu S, Majumdar A (2012) Opportunities and challenges for a sustainable energy future. Nature 488(7411):294–303
2. Turner JA (2004) Sustainable Hydrogen production. Science 305(5686):972–974. https://doi.org/10.1126/science.1103197
3. Walter MG, Warren EL, McKone JR, Boettcher SW, Mi Q, Santori EA, Lewis NS (2010) Solar water splitting cells. Chem Rev 110(11):6446–6473
4. Dresselhaus M, Thomas I (2001) Alternative energy technologies. Nature 414(6861):332–337
5. Zou X, Zhang Y (2015) Noble metal-free hydrogen evolution catalysts for water splitting. Chem Soc Rev 44(15):5148–5180. https://doi.org/10.1039/c4cs00448e
6. Pletcher D, Li X (2011) Prospects for alkaline zero gap water electrolysers for hydrogen production. Int J Hydrogen Energy 36(23):15089–15104
7. Reier T, Oezaslan M, Strasser P (2012) Electrocatalytic oxygen evolution reaction (OER) on Ru, Ir, and Pt catalysts: a comparative study of nanoparticles and bulk materials. ACS Catal 2(8):1765–1772
8. Ma W, Ma R, Wang C, Liang J, Liu X, Zhou K, Sasaki T (2015) A superlattice of alternately stacked Ni–Fe hydroxide nanosheets and graphene for efficient splitting of water. ACS Nano 9(2):1977–1984
9. Zhang B, Zheng X, Voznyy O, Comin R, Bajdich M, García-Melchor M, Han L, Xu J, Liu M, Zheng L, García de Arquer FP, Dinh CT, Fan F, Yuan M, Yassitepe E, Chen N, Regier T, Liu P, Li Y, De Luna P, Janmohamed A, Xin HL, Yang H, Vojvodic A, Sargent EH (2016) Homogeneously dispersed multimetal oxygen-evolving catalysts. Science 352(6283):333–337. https://doi.org/10.1126/science.aaf1525
10. Lu Z, Wang H, Kong D, Yan K, Hsu PC, Zheng G, Yao H, Liang Z, Sun X, Cui Y (2014) Electrochemical tuning of layered lithium transition metal oxides for improvement of oxygen evolution reaction. Nat Commun 5:4345. https://doi.org/10.1038/ncomms5345
11. Maiyalagan T, Jarvis KA, Therese S, Ferreira PJ, Manthiram A (2014) Spinel-type lithium cobalt oxide as a bifunctional electrocatalyst for the oxygen evolution and oxygen reduction reactions. Nat Commun 5:3949. https://doi.org/10.1038/ncomms4949
12. Liu Y-C, Koza JA, Switzer JA (2014) Conversion of electrodeposited $Co(OH)_2$ to CoOOH and Co_3O_4, and comparison of their catalytic activity for the oxygen evolution reaction. Electrochim Acta 140:359–365. https://doi.org/10.1016/j.electacta.2014.04.036
13. Zhou Y, Lee CW, Kim SK, Yoon S (2012) Ordered mesoporous carbon/MoO_2 nanocomposites as stable supercapacitor electrodes. ECS Electrochem Lett 1(1):A17–A20. https://doi.org/10.1149/2.013201eel
14. Gong M, Dai H (2014) A mini review of NiFe-based materials as highly active oxygen evolution reaction electrocatalysts. Nano Research 8(1):23–39. https://doi.org/10.1007/s12274-014-0591-z
15. Seh ZW, Kibsgaard J, Dickens CF, Chorkendorff I, Norskov JK, Jaramillo TF (2017) Combining theory and experiment in electrocatalysis: insights into materials design. Science 355(6321):eaad4998. https://doi.org/10.1126/science.aad4998
16. Huang J, Chen J, Yao T, He J, Jiang S, Sun Z, Liu Q, Cheng W, Hu F, Jiang Y, Pan Z, Wei S (2015) CoOOH nanosheets with high mass activity for water oxidation. Angew Chem Int Ed Engl 54(30):8722–8727. https://doi.org/10.1002/anie.201502836
17. Wang A-L, Xu H, Li G-R (2016) NiCoFe layered triple hydroxides with porous structures as high-performance electrocatalysts for overall water splitting. ACS Energy Lett 1(2):445–453. https://doi.org/10.1021/acsenergylett.6b00219
18. Jiang N, You B, Sheng M, Sun Y (2015) Electrodeposited cobalt-phosphorous-derived films as competent bifunctional catalysts for overall water splitting. Angew Chem Int Ed Engl 54(21):6251–6254. https://doi.org/10.1002/anie.201501616
19. Jiang N, You B, Sheng M, Sun Y (2016) Bifunctionality and mechanism of electrodeposited nickel-phosphorous films for efficient overall water splitting. ChemCatChem 8(1):106–112. https://doi.org/10.1002/cctc.201501150
20. Zhao S, Wang Y, Dong J, He C-T, Yin H, An P, Zhao K, Zhang X, Gao C, Zhang L, Lv J, Wang J, Zhang J, Khattak AM, Khan NA, Wei Z, Zhang J, Liu S, Zhao H, Tang Z (2016) Ultrathin metal–organic framework nanosheets for electrocatalytic oxygen evolution. Nature Energy 1:16184. https://doi.org/10.1038/nenergy.2016.184
21. Zhuang Z, Sheng W, Yan Y (2014) Synthesis of monodispere Au@Co_3O_4 core-shell nanocrystals and their enhanced catalytic activity for oxygen evolution reaction. Adv Mater 26(23):3950–3955. https://doi.org/10.1002/adma.201400336
22. Zhao Y, Chen S, Sun B, Su D, Huang X, Liu H, Yan Y, Sun K, Wang G (2015) Graphene-Co(3)O(4) nanocomposite as electrocatalyst with high performance for oxygen evolution reaction. Sci Rep 5:7629. https://doi.org/10.1038/srep07629
23. Han X, Yu C, Zhou S, Zhao C, Huang H, Yang J, Liu Z, Zhao J, Qiu J (2017) Ultrasensitive iron-triggered nanosized Fe-CoOOH integrated with graphene for highly efficient oxygen evolution. Adv Energy Mater. https://doi.org/10.1002/aenm.201602148
24. Shang C, Li M, Wang Z, Wu S, Lu Z (2016) Electrospun nitrogen-doped carbon nanofibers encapsulating cobalt nanoparticles as efficient oxygen reduction reaction catalysts. ChemElectroChem 3(9):1437–1445. https://doi.org/10.1002/celc.201600275
25. Liu Y, Liu Y, Cheng SH-S, Yu S, Nan B, Bian H, Md K, Wang M, Chung CY, Lu Z-G (2016) Conformal coating of heterogeneous CoO/Co nanocomposites on carbon nanotubes as efficient bifunctional electrocatalyst for Li-air batteries. Electrochim Acta 219:560–567. https://doi.org/10.1016/j.electacta.2016.10.064
26. Unni SM, Dhavale VM, Pillai VK, Kurungot S (2010) High Pt utilization electrodes for polymer electrolyte membrane fuel cells by dispersing Pt particles formed by a preprecipitation method on carbon “polished” with polypyrrole. J Phys Chem C 114(34):14654–14661. https://doi.org/10.1021/jp104664t
27. Bashyam R, Zelenay P (2006) A class of non-precious metal composite catalysts for fuel cells. Nature 443(7107):63–66. https://doi.org/10.1038/nature05118
28. Olson TS, Pylypenko S, Atanassov P, Asazawa K, Yamada K, Tanaka H (2010) Anion-exchange membrane fuel cells: dual-site mechanism of oxygen reduction reaction in alkaline media on cobalt–polypyrrole electrocatalysts. J Phys Chem C 114(11):5049–5059. https://doi.org/10.1021/jp910572g

29. Diallo A, Beye AC, Doyle TB, Park E, Maaza M (2015) Green synthesis of Co_3O_4 nanoparticles via *Aspalathus linearis*: physical properties. Green Chem Lett Rev 8(3–4):30–36. https://doi.org/10.1080/17518253.2015.1082646

30. Wang HY, Hung SF, Chen HY, Chan TS, Chen HM, Liu B (2016) In operando identification of geometrical-site-dependent water oxidation activity of spinel Co_3O_4. J Am Chem Soc 138(1):36–39. https://doi.org/10.1021/jacs.5b10525